

Cavity Dynamical Casimir Effect in the presence of three-level atom

A. V. Dodonov and V. V. Dodonov

Instituto de Física, Universidade de Brasília, PO Box 04455, 70910-900, Brasília, Distrito Federal, Brazil

We consider the scenario in which a damped three-level atom in the ladder or V configurations is coupled to a single cavity mode whose vacuum state is amplified by dint of the dynamical Casimir effect. We obtain approximate analytical expressions and exact numerical results for the time-dependent probabilities, demonstrating that the presence of the third level modifies the photon statistics and its population can serve as a witness of photon generation from vacuum.

PACS numbers: 42.50.Pq, 32.80.-t, 42.50.Ct, 42.50.Hz

I. INTRODUCTION

The physics of three-level quantum systems (“atoms”) interacting with quantized modes of electromagnetic field is very rich, and many special cases were studied in numerous papers (see, e.g., [1–12] and references therein). In the majority of studies, the coefficients of the Hamiltonians describing such systems were assumed time-independent. Time-dependent couplings were considered, e.g., in [13], but under the restriction of adiabatic variations. Here we consider the light-matter dynamics when a three-level atom interacts with a single cavity mode, whose frequency is rapidly modulated according to the harmonical law $\omega_t = \omega_0[1 + \varepsilon \sin(\eta t)]$ with a small modulation depth, $|\varepsilon| \ll 1$. We shall use dimensionless variables, setting $\hbar = \omega_0 = 1$. Such a situation can arise, in particular, if the selected mode describes the evolution of electromagnetic field in a cavity with vibrating walls, and one of the most impressive manifestations can be the so called Dynamical Casimir Effect (DCE), i.e., the photon generation from the initial vacuum state induced by the motion of boundaries [14, 15]. The simplest model describing this effect is based on the Hamiltonian

$$H_c = \omega_t n - i\chi_t (a^2 - a^{\dagger 2}), \quad (1)$$

where a and a^\dagger are the cavity annihilation and creation operators, and $n \equiv a^\dagger a$ is the photon number operator. The specific feature of the DCE is that two functions ω_t and χ_t are related as follows [16]:

$$\chi_t = (4\omega_t)^{-1} d\omega_t/dt, \quad (2)$$

If the modulation frequency η is close to the parametric resonance frequency, $\eta = 2(1+x)$ with $|x| \ll 1$, then one can expect an exponential growth of the mean number of photons inside the *empty ideal* cavity [17]. In particular, the mean number of photons created from the initial vacuum state for $x = 0$ equals

$$\langle n_0(t) \rangle = \sinh^2(\varepsilon t/2). \quad (3)$$

However, the situation can be very different if the field mode interacts with a detector while the cavity walls oscillate. For example, it was shown in [18] that no more than *two photons* can be created in the cavity if the

field-atom coupling is much stronger than the modulation depth ε . In view of the recent progress in experiments on simulating DCE [19–21], the detailed study of different detection schemes becomes a timely and important task.

Recently, various regimes of the *two-level* detectors were analyzed in [22–24]. On the other hand, *three-level* detectors can be more realistic [25], besides, they have several advantages [26]. Therefore we consider the evolution of the single-mode cavity field interacting with a three-level atom, whose free Hamiltonian is

$$H_a = \tilde{E}_1 \sigma_{11} + \tilde{E}_2 \sigma_{22} + \tilde{E}_3 \sigma_{33}, \quad (4)$$

(where \tilde{E}_i is the i th energy level, $|\mathbf{i}\rangle$ is the atomic energy eigenstate and $\sigma_{ij} \equiv |\mathbf{i}\rangle\langle\mathbf{j}|$). We are interested in the cases where the atom-field interaction modifies severely the atomless DCE. Therefore we assume that the $|\mathbf{1}\rangle \leftrightarrow |\mathbf{2}\rangle$ transition is resonant with the unperturbed cavity frequency, $\tilde{E}_2 = \tilde{E}_1 + 1$. Fig. 1 depicts two atomic level structures we consider here: the ladder (or Ξ) configuration and the V configuration, where $\Omega_2 \equiv \tilde{E}_3 - \tilde{E}_2$ and $\Omega_3 \equiv \tilde{E}_3 - \tilde{E}_1$ are the transition frequencies. We also define the detunings between the

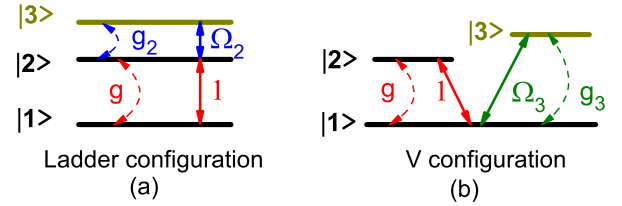


FIG. 1: (Color online) Diagram of the atomic configurations.

cavity unperturbed frequency and the other atomic transition frequency as $\Delta_2 \equiv 1 - \Omega_2$ and $\Delta_3 \equiv 1 - \Omega_3$. The set of constants g , g_2 and g_3 quantifies the atom-field dipolar coupling strengths between the energy levels as shown in Fig. 1. We assume these constants to be real and $\mathcal{O}(g_1) \sim \mathcal{O}(g_2) \sim \mathcal{O}(g_3)$ (although this is not the most general case, such a choice describes the main phenomena in the most simple way) and much smaller than unity. The corresponding light-matter interaction Hamiltonians are chosen in the standard Jaynes–Cummings form (i.e., we neglect the counter-rotating terms):

$$H_I^{(\Xi)} = a(g\sigma_{21} + g_2\sigma_{32}) + H.c., \quad (5)$$

$$H_I^{(V)} = a(g\sigma_{21} + g_3\sigma_{31}) + H.c., \quad (6)$$

where $H.c.$ stands for the Hermitian conjugate.

The questions we try to answer are: 1) how the presence of the third level can influence the number of created photons and the photon number distribution and 2) how big can the occupation probabilities of different levels be (this is important from the point of view of the detection of DCE). For this purpose we solved numerically the Schrödinger equation

$$d|\Psi\rangle/dt = -i(H_c + H_a + H_I)|\Psi\rangle \quad (7)$$

for the wavefunction of the total system, expanding this function over the atomic and Fock bases. Exact equations for the coefficients of this expansion were solved numerically using the Runge-Kutta-Verner fifth-order and sixth-order method, truncating the photon number space at the value $N = 196$. In this paper we focus on the amplification of the vacuum fluctuations, so we consider only the zero-excitation initial state, $|\Psi(0)\rangle = |1, 0\rangle$.

To be closer to realistic experimental conditions, we took into account in some cases (where the mean number of created photons was limited) a possibility of damping in the atomic degrees of freedom (but neglecting the dissipation in the field mode, assuming that the cavity quality factor is high enough), using the Lindblad-type Markovian master equation for the total statistical operator ρ of the atom-field system (in the ladder configuration)

$$\dot{\rho} = -i[H, \rho] + \lambda\mathfrak{D}[\sigma_{12}]\rho + \lambda_2\mathfrak{D}[\sigma_{23}]\rho, \quad (8)$$

where λ and λ_2 are the damping rates for the transitions $|2\rangle \rightarrow |1\rangle$ and $|3\rangle \rightarrow |2\rangle$, respectively, and the Lindblad kernel is

$$\mathfrak{D}[O]\rho \equiv (2O\rho O^\dagger - O^\dagger O\rho - \rho O^\dagger O)/2.$$

The maximal number of photons taken into account in such cases was $N = 7$ due to the necessity to calculate off-diagonal matrix elements not only in the atomic basis but also in the Fock one. We checked that the normalization conditions were fulfilled with an accuracy better than 10^{-10} in all the cases.

The results of numerical calculations are exposed in the next two sections together with some approximate analytical solutions clarifying them. We consider two typical situations: the strong atom-field coupling regime with $|g| \gg |\varepsilon|$ and the weak coupling regime with $|g| \ll |\varepsilon|$. Both these regimes could be implemented in the circuit QED realizations, where the values of g can be adjusted from very low values up to $|g| \sim 10^{-1}$ during fabrication or *in situ* [27]. The last section contains some discussion and conclusions.

II. LADDER CONFIGURATION

A. Main resonance for a strong field-atom coupling

In Fig. 2 we demonstrate the behavior of typical quantities characterizing the field and atom dynamics: the

average photon number $\langle n \rangle$, the atomic level populations σ_{ii} ($i = 1, 2, 3$) and the Mandel factor $Q = [\langle (\Delta n)^2 \rangle - \langle n \rangle] / \langle n \rangle$, for the resonance shift $x = 0$ and resonant third level in the absence of any damping and under the condition of strong field-atom coupling: $|\varepsilon| \ll |g|, |g_2|$. This case is especially interesting, because it gives the maximal photon generation rate for the empty cavity [17]. On the other hand, according to [18], there is no photon creation for $x = 0$ if the field mode interacts with a *two-level* atom under the condition $|\varepsilon| \ll |g|$.

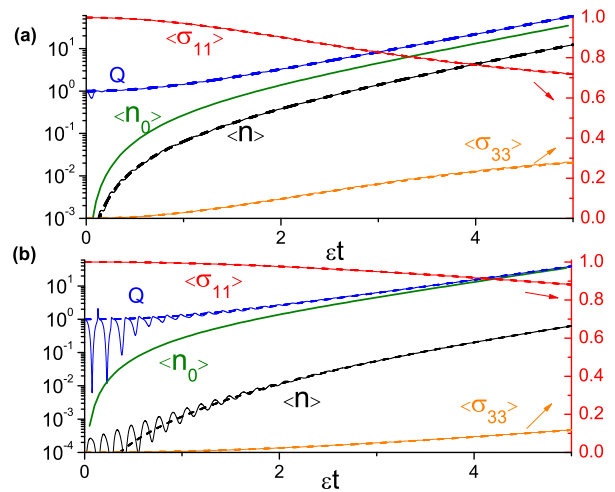


FIG. 2: (Color online) **a**) The behavior of different average values (described in the text) versus the dimensionless time εt in the strong modulation regime for $x = 0$ and the following values of other parameters: **a**) $\lambda = \Delta_2 = 0$, $g = 3 \times 10^{-2}$, $g_2 = 4 \times 10^{-2}$, $\varepsilon = 10^{-3}$; **b**) the same as (a) but for $g_2 = 10^{-2}$.

Solid lines correspond to exact numerical results and the dashed ones – to the approximation based on Eqs. (21)-(23) deduced below. We see that for $\varepsilon t > 1$ the mean number of photons grows exponentially with the same increment $d \ln \langle n \rangle / dt$ as in the empty-cavity case described by Eq. (3), although $\langle n \rangle$ can be much less than $\langle n_0 \rangle$ if $g_2 < g$.

To understand qualitatively how the coupling with the third level changes the system dynamics we used the following chain of approximations. In the weak modulation case $|\varepsilon| \ll 1$ considered here, one can write $\chi_t \simeq 2q \cos(\eta t)$ with $q \equiv \varepsilon(1+x)/4$. Going to the interaction picture via the transformation $|\Psi(t)\rangle = V(t)|\psi(t)\rangle$, with $V(t) = \exp[-it(\eta/2)(n + \sigma_{33} - \sigma_{11})]$, and performing the Rotating Wave Approximation (RWA), one obtains the approximate *time-independent* Hamiltonian governing the time evolution of $|\psi(t)\rangle$

$$H_1 \simeq (ga\sigma_{21} + g_2a\sigma_{32} - iqa^2 + H.c.) + x(\sigma_{11} - n - \sigma_{33}) - \Delta_2\sigma_{33}. \quad (9)$$

It is convenient to expand the function $|\psi(t)\rangle$ over the

atomic and Fock basis as follows:

$$|\psi(t)\rangle = \sum_{n=0}^{\infty} e^{inx} (e^{-itx} p_{1n} |\mathbf{1}, n\rangle + p_{2n} |\mathbf{2}, n\rangle + e^{it(x+\Delta_2)} p_{3n} |\mathbf{3}, n\rangle), \quad (10)$$

so that $|p_{in}|^2$ is the probability of the atom to be in the \mathbf{i} -th state with the field having n photons. The time-dependent phase factors are introduced here to simplify the equations for the coefficients p_{in} . Putting (10) into the equation $d|\psi\rangle/dt = -iH_1|\psi\rangle$ we obtain the following differential equations for the probability amplitudes:

$$\dot{p}_{1n} = -i\sqrt{n}gp_{2(n-1)} + \mathcal{W}_1(n) \quad (11)$$

$$\dot{p}_{2n} = -ig\sqrt{n+1}p_{1(n+1)} - ig_2\sqrt{n}e^{i\Delta_2 t}p_{3(n-1)} + \mathcal{W}_2(n) \quad (12)$$

$$\dot{p}_{3n} = -ig_2\sqrt{n+1}e^{-i\Delta_2 t}p_{2(n+1)} + \mathcal{W}_3(n), \quad (13)$$

where for $\mathbf{i} = \mathbf{1}, \mathbf{2}, \mathbf{3}$

$$\mathcal{W}_i(n) \equiv q \left[\sqrt{n(n-1)}e^{-2ixt}p_{i(n-2)} - \sqrt{(n+1)(n+2)}e^{2ixt}p_{i(n+2)} \right]. \quad (14)$$

Analyzing Eqs. (11)-14) one can see that for the initial state $|\mathbf{1}, 0\rangle$ the only nonzero coefficients at $t > 0$ can be $p_{1(2k)}$, $p_{2(2k+1)}$, and $p_{3(2k)}$, with $k = 0, 1, 2, \dots$

For $|\varepsilon| \ll |g|$ we follow the scheme used in [18, 22]. First we solve Eqs. (11)-(13) for $q = 0$ (i.e., in the stationary cavity). In the strict resonant case, $\Delta_2 = 0$, we have $p_{10}(t) = \text{const}$, whereas for $n = 2, 4, 6, \dots$ the solutions can be written as follows:

$$p_{1n} = \frac{g\sqrt{n}}{G_n} (A_n e^{-iG_n t} - B_n e^{iG_n t} - C_n), \quad (15)$$

$$p_{3(n-2)} = \frac{g_2\sqrt{n-1}}{G_n} \left[A_n e^{-iG_n t} - B_n e^{iG_n t} + \frac{ng^2 C_n}{(n-1)g_2^2} \right] \quad (16)$$

$$p_{2(n-1)} = A_n e^{-iG_n t} + B_n e^{iG_n t}, \quad (17)$$

where $G_n \equiv \sqrt{ng^2 + (n-1)g_2^2}$ and constants A_n, B_n, C_n are determined by the initial conditions. For $q \neq 0$ we put expressions (15)-(17) into Eqs. (11)-(13), obtaining the equivalent equations $\dot{p}_{10} = -q\sqrt{2}e^{2ixt}p_{12}$ and for $n \geq 2$

$$\dot{A}_n e^{-iG_n t} - \dot{B}_n e^{iG_n t} - \dot{C}_n = \frac{G_n}{g\sqrt{n}} \mathcal{W}_1(n) \quad (18)$$

$$\dot{A}_n e^{-iG_n t} - \dot{B}_n e^{iG_n t} + \frac{ng^2 \dot{C}_n}{(n-1)g_2^2} = \frac{G_n \mathcal{W}_3(n-2)}{g_2\sqrt{n-1}} \quad (19)$$

$$\dot{A}_n e^{-iG_n t} + \dot{B}_n e^{iG_n t} = \mathcal{W}_2(n-1). \quad (20)$$

According to numerical results, all coefficients p_{2n} are very small for $x = 0$. Therefore we neglect functions $A_n(t)$ and $B_n(t)$ in all terms, except for the left-hand sides of Eqs. (18) and (19), because the derivatives \dot{A}_n and \dot{B}_n can be not small due to fast oscillations of these functions with the frequencies of the order of G_n . To eliminate these derivatives we take the difference of equations (18) and (19), arriving at the set of equations containing only coefficients C_n — here we make the approximation, removing $A_n(t)$ and $B_n(t)$ from the terms $\mathcal{W}_1(n)$ and $\mathcal{W}_3(n)$. After that we rewrite the coefficients C_n in terms of p_{1n} according to Eq. (15) with neglected $A_n(t)$ and $B_n(t)$. Thus we obtain the following infinite set of differential equations coupling the functions p_{1n} only:

$$\dot{p}_{10} = -(\varepsilon/4)\sqrt{2}p_{12}, \quad (21)$$

$$\dot{p}_{12} = (\varepsilon/4) \left[\frac{g_2^2\sqrt{2}}{G_2^2} p_{10} - \frac{2\tilde{G}_2^2}{\sqrt{3}G_2^2} p_{14} \right], \quad (22)$$

$$\dot{p}_{1n} = (\varepsilon/4)(n-1) \left[\sqrt{\frac{n}{n-1}} \frac{\tilde{G}_{n-2}^2}{G_n^2} p_{1(n-2)} - \sqrt{\frac{n+2}{n+1}} \frac{\tilde{G}_n^2}{G_n^2} p_{1(n+2)} \right], \quad (23)$$

where $\tilde{G}_n \equiv \sqrt{ng^2 + (n+1)g_2^2}$ and $n = 4, 6, \dots$. The amplitudes p_{3n} can be calculated by means of the relation

$$p_{3n} \simeq -(g/g_2)\sqrt{(n+2)/(n+1)}p_{1(n+2)}, \quad (24)$$

which follows from Eq. (12) if one puts $p_{2n} \approx 0$ there.

Although equations (21)-(23) cannot be solved analytically due to the presence of various square roots in the coefficients, they are very useful, both for numerical calculations and the qualitative analysis. Fig. 2 shows that differences between exact solutions of the full Schrödinger equation (7) and the approximate ones based on the set (21)-(23) practically disappear in the most interesting regime $\varepsilon t > 1$. But solving (21)-(23) numerically requires much less resources than solving (7), therefore using (21)-(23) we can calculate the amplitudes for much bigger values of the dimensionless time εt . In this way we confirmed numerically that the exponential growth of the mean photon number continues (at least for $\varepsilon t \lesssim 10$). The population of the second level shows fast oscillations, not exceeding the values of the order of $(\varepsilon/g)^2$, as can be evaluated from Eqs. (17) and (18).

The order of magnitude of amplitudes p_{1n} with $n \geq 2$ is determined by the coefficient $(g_2/G_2)^2$ at the first term in the right-hand side of Eq. (22) (the common coefficient ε in Eqs. (21)-(23) determines the time scale εt of the evolution of the photon subsystem, as well as the atomic 1st and 3rd levels). If $|g_2| \ll |g|$, then $|p_{1n}|^2 \sim (g_2/g)^4$ for $n \geq 2$, whereas $|p_{3n}|^2 \sim (g_2/g)^2$ for $n \geq 0$, due to Eq. (24), so that the process of photon generation is correlated with the population of the third level. In particular,

for $g_2 = 0$ (the two-level system) the coefficient p_{12} is not coupled to p_{10} in Eq. (22) at the initial moment, so that $p_{1n}(t) \equiv 0$ for $n \geq 2$, meaning that photons cannot be generated in accordance with [18, 22].

In the opposite limit $|g_2| \gg |g|$ we have $\tilde{G}_{n-2}^2/G_n^2 \approx 1$ and $\tilde{G}_n^2/G_n^2 \approx (n+1)/(n-1)$. Therefore Eqs. (21)-(23) become identical with the equations for the photon generation in the empty cavity (without atoms) given, e.g. by Eq. (11) with $g = x = 0$. In this case $|p_{3n}|^2 \sim \sigma_{33} \sim (g/g_2)^2 \ll 1$. It looks like the three-level atom becomes “invisible” for the field if $|g_2| \gg |g|$.

Note that the Mandel Q -factor is always positive in Fig. 2, moreover, it increases with the same increment as the mean photon number for $\varepsilon t > 1$, being always much bigger than $\langle n \rangle$. This means that the photon number fluctuations are rather strong and the photon statistics is “hyper-Poissonian”, similar to the two-level case [23].

B. Resonances with creation of two photons

Looking at equations (18)-(20) one can see that choosing certain nonzero values of the resonance shift x [contained in the functions $\mathcal{W}_i(n)$] one can reduce the arguments of some exponentials in these equations to zero values, whilst other exponentials will oscillate with large arguments. In such cases we can perform the RWA and obtain a smaller set of essentially resonantly coupled differential equations. In particular, simple solutions for $\Delta_2 = 0$ arise if $2x = \pm G_2$. Then only four probabilities can be significantly different from zero:

$$|p_{10}|^2 \simeq \cos^2(\nu t), \quad |p_{12}|^2 \simeq \frac{g^2}{G_2^2} \sin^2(\nu t), \quad (25)$$

$$|p_{21}|^2 \simeq \frac{1}{2} \sin^2(\nu t), \quad |p_{30}|^2 \simeq \frac{g_2^2}{2G_2^2} \sin^2(\nu t), \quad (26)$$

where $\nu \equiv \sqrt{2}gq/G_2$ and $G_2 = \sqrt{2g^2 + g_2^2}$. All other probabilities contain extra factors of the order of $(\varepsilon/g)^2$, so they can be neglected in this approximation. We see that at most two photons can be generated with a significant probability and the third level becomes partially populated (if $g_2 = 0$, then the results coincide with that obtained in [18]). A similar effect of an indirect interaction between different energy levels was discovered in [28], where the *coupling constants* depended on the time-dependent cavity length $L(t)$ as $g \sim [L(t)]^{-1/2}$, while the cavity frequency was supposed to be constant. One more analog is the effect of “atomic shaking” in cavities with moving boundaries, studied in [29]. Recently, an analog of DCE in three-level systems with time-dependent Rabi frequencies was considered in [30]. We have verified that simple analytical formulas (25)–(26) are in full agreement with exact results obtained by solving numerically the Schrödinger equation (7) (the difference turns out to be less than the thickness of lines used in the plots).

However, simple formulas (26) hold only in the absence of dissipation. In Fig. 3a we show numerical results for

nonvanishing probabilities for parameters: $\Delta_2 = 0$, $g = 3 \times 10^{-2}$, $g_2 = 4 \times 10^{-2}$, $\varepsilon = 10^{-3}$ and the resonant shift $2x = G_2$, setting $\lambda = 5 \times 10^{-4}$ and $\lambda_2 = \lambda(g_2/g)^2$; such a choice agrees with a concrete example of the transmon multi-level qubit considered in [27] (assuming that the noise couples to the atom via the dipolar interaction [31]). One can see that although no more than two photons can be created from vacuum, there are no oscillations predicted by Eq. (26). Moreover, the probabilities $|p_{20}|^2$ and $|p_{11}|^2$ become different from zero due to the influence of dissipation.

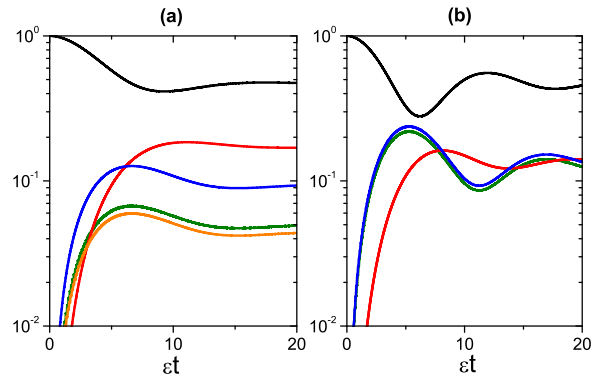


FIG. 3: (Color online) Dynamics of nonzero probabilities for the ladder configuration and nonzero resonance shifts. The order of curves at $\varepsilon t = 10$ is as follows (from above). For $2x = G_2$ (part a): $|p_{10}|^2$, $|p_{20}|^2$ (coincident with $|p_{11}|^2$), $|p_{21}|^2$, $|p_{12}|^2$ and $|p_{30}|^2$. For $2x = \delta_2/2 + J$ (part b): $|p_{10}|^2$, $|p_{20}|^2$ (coincident with $|p_{11}|^2$), $|p_{21}|^2$, $|p_{12}|^2$. The values of parameters are given in the text.

For the stationary cavity ($q = 0$) in the *dispersive case*, $|\Delta_2| \gg |g_2|$, one can write $p_{30} \simeq (g_2/\Delta_2) e^{-i\Delta_2 t} p_{21}$. After repeating the same steps as above we find that for $2x = \delta_2/2 \pm J$ (where $\delta_2 \equiv g_2^2/\Delta_2$ is the dispersive shift due to the third level and $J \equiv \sqrt{\delta_2^2/4 + 2g^2}$) the only nonzero probabilities are

$$\begin{aligned} |p_{10}|^2 &\simeq \cos^2(q\nu_{\mp} t), & |p_{12}|^2 &\simeq \frac{1}{2} \nu_{\mp}^2 \sin^2(q\nu_{\mp} t), \\ |p_{21}|^2 &\simeq \frac{1}{2} \nu_{\pm}^2 \sin^2(q\nu_{\mp} t), & |p_{30}|^2 &\simeq \frac{g_2^2}{\Delta_2^2} |p_{21}|^2, \end{aligned} \quad (27)$$

where $\nu_{\pm} = \sqrt{1 \pm \delta_2/(2J)}$. Thus, the rate of photon generation and the occupation probabilities are influenced by the level $|3\rangle$, although it remains effectively unpopulated for all times, as was confirmed by numerical simulations. In Fig. 3b we show the probabilities obtained from the numerical solution of the master equations for $\Delta_2 = 10g_2$, resonance shift $2x = \delta_2/2 + J$ and other parameters as in Fig. 3a. As expected, the third level is effectively unpopulated and $|p_{21}|^2$ is slightly bigger than $|p_{12}|^2$, in accordance with the predictions given in Eq. (27) for the dissipationless case. Some traces of oscillations are also visible here. They are more pronounced for smaller values of parameter λ .

C. Weak field-atom coupling

For a weak field-atom coupling, $|\varepsilon| \gg |g|$, many photons can be generated under the resonance condition $x = 0$. To calculate the accompanying atomic dynamics in this case, it is convenient to use the effective Hamiltonian approach instead of solving the differential equations for the probability amplitudes [23]. For this purpose we write the time-dependent state $|\psi(t)\rangle$ governed by the Hamiltonian H_1 as

$$|\psi(t)\rangle = e^{-iH_1 t} |\psi(0)\rangle = U^\dagger \exp(-iH_{ef}t) U |\psi(0)\rangle, \quad (28)$$

where $|\psi(0)\rangle$ is the initial state and we introduced a unitary operator U to define the effective Hamiltonian $H_{ef} \equiv UH_1U^\dagger$. In the resonant regime, $\Delta_2 = 0$, we choose the transformation [24]

$$U = e^{iY}, \quad Y = a^\dagger (\xi\sigma_{21} + \xi_2\sigma_{32}) + a (\xi\sigma_{12} + \xi_2\sigma_{23}), \quad (29)$$

where $\xi = 2g/\varepsilon \ll 1$ and $\xi_2 = 2g_2/\varepsilon \ll 1$. Then to the second order in ξ

$$H_{ef} = i\theta (a^{\dagger 2} - a^2) + iq\xi\xi_2 (\sigma_{13} - \sigma_{31}), \quad (30)$$

where $\theta \equiv q[1 + \xi^2(\sigma_{22} - \sigma_{11}) + \xi_2^2(\sigma_{33} - \sigma_{22})]$ is an operator with respect to the atomic basis. This effective Hamiltonian holds approximately for $|g|t \ll 1$, so the product $|\varepsilon|t$ can be greater than unity and several photons can be created from vacuum. We can write

$$\exp(-iH_{ef}t) = \hat{\Lambda}_s \exp\{iqt[\alpha_z(\sigma_{33} - \sigma_{11})/2 + i\xi\xi_2(\sigma_{31} - \sigma_{13})]\}, \quad (31)$$

where $\hat{\Lambda}_v \equiv \exp[vt(a^{\dagger 2} - a^2)]$ is the squeezing operator with nonzero matrix elements in the Fock basis [32]

$$\Lambda_v^{(n)} \equiv \langle 2n | \hat{\Lambda}_v | 0 \rangle = C_v^{-1/2} (S_v/C_v)^n \frac{\sqrt{(2n)!}}{2^n n!}.$$

Here $C_v \equiv \cosh(2vt)$ and $S_v \equiv \sinh(2vt)$. The operator α_z and index s of the operator $\hat{\Lambda}_s$ in (31) have the form

$$\begin{aligned} \alpha_z &= -i(\xi^2 + \xi_2^2)(a^{\dagger 2} - a^2), \\ s &= q[1 + (\xi^2 - \xi_2^2)(3\sigma_{22} - 1)/2]. \end{aligned}$$

After disentangling the second exponential in Eq. (31) according to [32], using the property $\hat{\Lambda}_v a \hat{\Lambda}_v^\dagger = C_v a - S_v a^\dagger$ one can show that for the initial state $|\psi(0)\rangle = |\mathbf{1}, 0\rangle$ the occupation probabilities to the *second order* in ξ can be written as follows:

$$\begin{aligned} |\langle \mathbf{1}, 2n | \psi(t) \rangle|^2 &= [1 - 2\xi^2(n+1)] \Lambda_{\theta_1}^{(n)2} \\ &+ \Lambda_{\theta_1}^{(n)} \left[2\xi^2(2n+1) C_{\theta_2}^{-1} \Lambda_{\theta_2}^{(n)} \right. \\ &\left. - (\xi^2 + \xi_2^2) qt (4n S_{\theta_1}^{-1} - S_{\theta_1} C_{\theta_1}^{-1}) \Lambda_{\theta_1}^{(n)} \right] \end{aligned}$$

$$|\langle \mathbf{2}, 2n+1 | \psi(t) \rangle|^2 = \xi^2(2n+1) \left(C_{\theta_2}^{-1} \Lambda_{\theta_2}^{(n)} - \Lambda_{\theta_1}^{(n)} \right)^2,$$

$$\theta_1 = q[1 - (\xi^2 - \xi_2^2)/2], \quad \theta_2 = q[1 + (\xi^2 - \xi_2^2)].$$

The amplitudes related to the third level are very small: $|\langle \mathbf{3}, 2n | \psi(t) \rangle|^2 \propto (\xi\xi_2)^2$ (and other probability amplitudes are exactly zero due to the assumed initial state $|\mathbf{1}, 0\rangle$). Therefore, in the resonant regime the third level is not populated within the time scale $gt \lesssim 1$, but the photon statistics is nevertheless slightly modified due to the presence of ξ_2 in the formulas. We checked these expressions by solving numerically the Schrödinger equation (7) and found an excellent agreement.

III. V CONFIGURATION

Now we repeat the steps of the previous section for the atom-field interaction Hamiltonian (6) that describes the atomic configuration depicted in Fig. 1b. Using the transformation $|\Psi(t)\rangle = V(t)|\psi(t)\rangle$ with $V(t) = \exp[-it(\eta/2)(n + \sigma_{33} + \sigma_{22})]$ we obtain

$$\begin{aligned} H_2 &\simeq (ga\sigma_{21} + g_3a\sigma_{31} - iqa^2 + H.c.) \\ &\quad - x(n + \sigma_{22} + \sigma_{33}) - \Delta_3\sigma_{33}. \end{aligned}$$

Only the states $\{|\mathbf{1}, 2n\rangle, |\mathbf{2}, 2n-1\rangle, \text{ and } |\mathbf{3}, 2n-1\rangle\}$ are populated ($n \geq 1$) during the unitary evolution for the initial state $|\mathbf{1}, 0\rangle$. Writing the wavefunction as

$$\begin{aligned} |\psi\rangle &= \sum_{n=0} e^{ixnt} (p_{1n} |\mathbf{1}, n\rangle + e^{itx} p_{2n} |\mathbf{2}, n\rangle \\ &\quad + e^{it(\Delta_3+x)} p_{3n} |\mathbf{3}, n\rangle), \end{aligned}$$

we obtain the equations

$$\begin{aligned} \dot{p}_{1n} &= -ig\sqrt{n} p_{2(n-1)} - ig_3\sqrt{n} e^{it\Delta_3} p_{3(n-1)} + \mathcal{W}_1(n), \\ \dot{p}_{2n} &= -ig\sqrt{n+1} p_{1(n+1)} + \mathcal{W}_2(n), \\ \dot{p}_{3n} &= -ig_3\sqrt{n+1} e^{-it\Delta_3} p_{1(n+1)} + \mathcal{W}_3(n). \end{aligned}$$

Their solutions for $\Delta_3 = q = 0$ are

$$p_{1n} = A_n e^{-iG_n t} + B_n e^{iG_n t}, \quad (32)$$

$$p_{2(n-1)} = \frac{g\sqrt{n}}{G_n} (A_n e^{-iG_n t} - B_n e^{iG_n t} + C_n),$$

$$p_{3(n-1)} = \frac{g_3\sqrt{n}}{G_n} \left(A_n e^{-iG_n t} - B_n e^{iG_n t} - \frac{g^2}{g_3^2} C_n \right), \quad (33)$$

where $G_n \equiv \sqrt{n(g^2 + g_3^2)}$. Therefore for the *weak modulation* ($|\varepsilon| \ll |g|$) the resonances occur for $2x = \pm G_n$ only, resulting in the probabilities

$$|p_{10}|^2 \simeq \cos^2(qt), \quad |p_{12}|^2 \simeq \frac{1}{2} \sin^2(qt), \quad (34)$$

$$|p_{21}|^2 \simeq \frac{g^2}{G_2^2} \sin^2(qt), \quad |p_{31}|^2 \simeq \frac{g_3^2}{G_2^2} \sin^2(qt). \quad (35)$$

Moreover, since p_{12} does not contain the coefficient C_2 in Eq. (32), the $x = 0$ resonance does not appear for the V configuration. In the dispersive regime, $|\Delta_3| \gg |g_3|$, one can write $p_{31} \simeq (\sqrt{2}g_3/\Delta_3)e^{-it\Delta_3}p_{12}$, where $\delta_3 \equiv g_3^2/\Delta_3$, and we find that the resonances occur for $2x = \delta_3 \pm J$ with resulting probabilities

$$\begin{aligned} |p_{10}|^2 &\simeq \cos^2(q\nu_{\pm}t), & |p_{12}|^2 &\simeq \frac{1}{2}\nu_{\pm}^2 \sin^2(q\nu_{\pm}t) \\ |p_{21}|^2 &\simeq \frac{1}{2}\nu_{\mp}^2 \sin^2(q\nu_{\pm}t), & |p_{31}|^2 &\simeq \frac{2g_3^2}{\Delta_3^2} |p_{12}|^2 \end{aligned} \quad (36)$$

where $J \equiv \sqrt{\delta_3^2 + 2g^2}$ and $\nu_{\pm} = \sqrt{1 \pm \delta_3/J}$. Notice that the expressions (36) are slightly different from the corresponding expressions (27) for the ladder configuration.

For the *strong modulation*, $|\varepsilon| \gg |g|$, we perform the transformation

$$U = e^{iY}, \quad Y = a^\dagger (\xi\sigma_{21} + \xi_3\sigma_{31}) + a (\xi\sigma_{12} + \xi_3\sigma_{13}), \quad (37)$$

where $\xi = 2g/\varepsilon \ll 1$ and $\xi_3 = 2g_3/\varepsilon \ll 1$, to obtain the effective Hamiltonian in the resonant regime (valid for $t \ll |g|^{-1}$ to the second order in ξ)

$$H_{ef} = i[\theta + q\xi\xi_3(\sigma_{23} + \sigma_{32})](a^{\dagger 2} - a^2), \quad (38)$$

where $\theta \equiv q[1 + \xi^2(\sigma_{22} - \sigma_{11}) + \xi_3^2(\sigma_{33} - \sigma_{11})]$. After disentangling $\exp(-iH_{ef}t)$ we get the following nonvanishing probabilities for the initial state $|\mathbf{1}, 0\rangle$:

$$\begin{aligned} |\langle \mathbf{1}, 2n | \psi(t) \rangle|^2 &= [1 - 2(\xi^2 + \xi_3^2)(n+1)] \Lambda_{\theta_1}^{(n)2} \\ &\quad + 2(2n+1)(\xi^2 + \xi_3^2) C_{\theta_2}^{-1} \Lambda_{\theta_2}^{(n)} \Lambda_{\theta_1}^{(n)}, \end{aligned}$$

$$|\langle \mathbf{2}, 2n+1 | \psi(t) \rangle|^2 = \xi^2 (2n+1) \left(C_{\theta_2}^{-1} \Lambda_{\theta_2}^{(n)} - \Lambda_{\theta_1}^{(n)} \right)^2,$$

$$|\langle \mathbf{3}, 2n+1 | \psi(t) \rangle|^2 = \xi_3^2 (2n+1) \left(C_{\theta_2}^{-1} \Lambda_{\theta_2}^{(n)} - \Lambda_{\theta_1}^{(n)} \right)^2,$$

where $\theta_1 = q(1 - \xi^2 - \xi_3^2)$ and $\theta_2 = q[1 + (\xi^2 + \xi_3^2)/2]$. As expected for the resonant regime, the third level can be substantially populated in this case, and the photon statistics is severely modified as compared to the scenario of resonant two-level atom.

In Fig. 4 we illustrate the exact dynamics for the V configuration. Fig. 4a shows the behavior of probabilities in the resonant regime ($\Delta_3 = 0$) and weak modulation ($\varepsilon = 10^{-3}$) for $2x = G_2$, while in Fig. 4b we consider the dispersive regime ($\Delta_3 = -12g_3$) and the resonance shift $2x = \delta_3 + J$. We included atomic damping by means of the master equation (8), replacing the term $\lambda_2 \mathcal{D}[\sigma_{23}] \rho$ by $\lambda_3 \mathcal{D}[\sigma_{13}] \rho$, where λ_3 is that for the transition $|\mathbf{3}\rangle \rightarrow |\mathbf{1}\rangle$ [other parameters are: $g = 3 \times 10^{-2}$, $g_3 = 4 \times 10^{-2}$, $\lambda = 5 \times 10^{-4}$, $\lambda_3 = \lambda(g_3/g)^2$]. In both cases at most two photons are created as predicted analytically in the absence of damping, and in the dispersive case $|p_{21}|^2$ lies slightly above $|p_{12}|^2$ in accordance with Eq. (36). In

Fig. 4c we show the photon distribution (obtained by tracing out the atomic degrees of freedom) in the absence of damping for $x = 0$ in the strong modulation regime for parameters $\varepsilon = 10^{-2}$, $g = 5 \times 10^{-4}$, $g_3 = 8 \times 10^{-4}$ and $\Delta_3 = -4g_3$ (so the third level is neither in resonant nor in dispersive regime). For comparison we show the photon number distribution in the absence of the third level ($g_3 = 0$) to emphasize that the photon statistics is substantially modified due to the interaction with the third level.

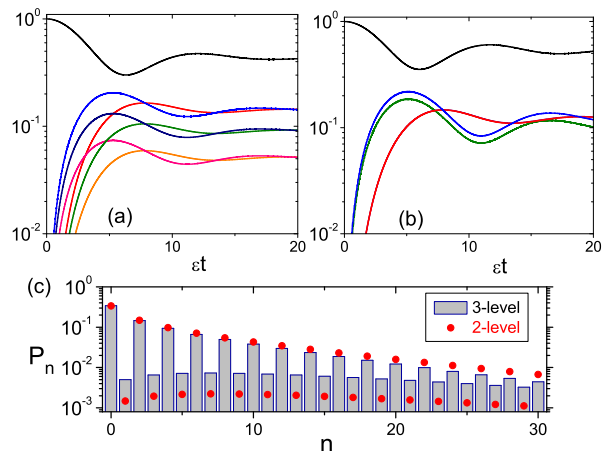


FIG. 4: (Color online) Atom-field dynamics for the V configuration and different resonance shifts. The order of curves at $et = 10$ is as follows (from above). **a**) For $2x = G_2$: $|p_{10}|^2$, $|p_{11}|^2$, $|p_{12}|^2$, $|p_{30}|^2$, $|p_{31}|^2$, $|p_{20}|^2$, $|p_{21}|^2$. **b**) For $2x = \delta_3 + J$: $|p_{10}|^2$, $|p_{11}|^2$ (coincident with $|p_{20}|^2$), $|p_{21}|^2$, $|p_{12}|^2$. **c**) Photon number distribution for $x = 0$ and $et = 3.5$ in the strong modulation regime and $\Delta_3 = -4g_3$ (without damping, $\lambda = \lambda_3 = 0$), compared to the two-level atom case ($g_3 = 0$). The values of other parameters are given in the text.

IV. CONCLUSIONS

We presented results of exact numerical calculations for the atom-field dynamics when a three-level atom (see Fig. 1) interacts with a single cavity field mode whose vacuum state is being amplified via the dynamical Casimir effect. In some cases we succeeded to find simple analytical expressions explaining these results. This study is relevant since the actual atoms in cavity QED and artificial atoms in circuit QED are indeed multi-level systems. We found that the third level modifies the resonance frequencies as compared to the two-level case, and the dynamical behavior may be drastically different from the cases of atomless cavity or a two-level atom. The results obtained might be useful for the design of schemes aimed at the detection of the Casimir photons by measuring the occupancies of different atomic levels. For instance, the modulation frequency equal to twice the unperturbed cavity frequency does lead to photon generation from vacuum and occupation of the third level

in the ladder configuration, whereas this modulation frequency is forbidden in the case of two-level resonant atom or V configuration. This could facilitate the experiment, because there is no need in such a case to adjust the resonance frequency shift, knowing that the main resonance must happen exactly at twice the frequency of the unperturbed cavity mode, while the occupancy of the third level in the ladder configuration can serve as a witness of the photon generation, because whenever the photons are generated the third level becomes populated. In any case, the inclusion of the third level provides an opportunity for observing a rich dynamical behavior. Also, the three-level schemes can be useful for the creation of different

entangled states between the field and atoms (whereas by using post-selection methods based on detecting the atomic state, novel cavity field states could be engineered [23]).

Acknowledgments

A.V.D. acknowledges the partial support of DPP/UnB. V.V.D. acknowledges the partial support of CNPq (Brazilian agency).

-
- [1] P. L. Knight and P. W. Milonni, *Phys. Rep.* **66**, 21 (1980).
- [2] H.-I. Yoo and J. H. Eberly, *Phys. Rep.* **118**, 239 (1985).
- [3] S. M. Chumakov, V. V. Dodonov, and V. I. Man'ko, in *Classical and Quantum Effects in Electrodynamics*, edited by A. A. Komar, Proc. Lebedev Phys. Inst. Vol. 176 (Nova Science, Commack, New York, 1988), p. 77.
- [4] V. Bužek, *J. Mod. Opt.* **37**, 1033 (1990).
- [5] C. C. Gerry and J. H. Eberly, *Phys. Rev. A* **42**, 6805 (1990).
- [6] Fam Le Kien and A. S. Shumovsky, *Int. J. Mod. Phys. B* **5**, 2287 (1991).
- [7] M. Alexanian and S. K. Bose, *Phys. Rev. A* **52**, 2218 (1995).
- [8] Ying Wu and Xiaoxue Yang, *Phys. Rev. A* **56**, 2443 (1997).
- [9] Jing-Bo Xu and Xu-Bo Zou, *Phys. Rev. A* **60**, 4743 (1999).
- [10] A. B. Klimov and L. L. Sanchez-Soto, *Phys. Rev. A* **61**, 063802 (2000).
- [11] M. Fleischhauer and M. D. Lukin, *Phys. Rev. A* **65**, 022314 (2002).
- [12] A. Messina, S. Maniscalco, and A. Napoli, *J. Mod. Opt.* **50**, 1 (2003).
- [13] M. Janowicz, *Phys. Rep.* **375**, 327 (2003).
- [14] V. V. Dodonov, *Phys. Scr.* **82**, 038105 (2010).
- [15] D. A. R. Dalvit, P. A. Maia Neto, and F. D. Mazzitelli, in *Casimir Physics*, edited by D. Dalvit, P. Milonni, D. Roberts, and F. da Rosa, Lecture Notes in Physics Vol. 834 (Springer, Berlin, 2011), p. 419.
- [16] C. K. Law, *Phys. Rev. A* **49**, 433 (1994).
- [17] V. V. Dodonov and A. B. Klimov, *Phys. Rev. A* **53**, 2664 (1996); G. Plunien, R. Schützhold, and G. Soff, *Phys. Rev. Lett.* **84**, 1882 (2000); M. Croce, D. A. R. Dalvit, and F. D. Mazzitelli, *Phys. Rev. A* **64**, 013808 (2001).
- [18] V. V. Dodonov, *Phys. Lett. A* **207**, 126 (1995).
- [19] C. M. Wilson, G. Johansson, A. Pourkabirian, M. Simoen, J. R. Johansson, T. Duty, F. Nori, and P. Delsing, *Nature (London)* **479**, 376 (2011).
- [20] P. D. Nation, J. R. Johansson, M. P. Blencowe, and F. Nori, *Rev. Mod. Phys.* **84**, 1 (2012).
- [21] A. Agnesi, C. Braggio, G. Carugno, F. Della Valle, G. Galeazzi, G. Messineo, F. Pirzio, G. Reali, and G. Ruoso, *Rev. Sci. Instr.* **82**, 115107 (2011).
- [22] A. V. Dodonov, R. Lo Nardo, R. Migliore, A. Messina, and V. V. Dodonov, *J. Phys. B* **44**, 225502 (2011).
- [23] A. V. Dodonov and V. V. Dodonov, *Phys. Lett. A* **375**, 4261 (2011).
- [24] A. V. Dodonov and V. V. Dodonov, *Phys. Rev. A* **85**, 015805 (2012).
- [25] B. Peropadre, G. Romero, G. Johansson, C. M. Wilson, E. Solano, and J. J. García-Ripoll, *Phys. Rev. A* **84**, 063834 (2011).
- [26] D. Pinotsi and A. Imamoglu, *Phys. Rev. Lett.* **100**, 093603 (2008).
- [27] J. Koch, T. M. Yu, J. Gambetta, A. A. Houck, D. I. Schuster, J. Majer, A. Blais, M. H. Devoret, S. M. Girvin, and R. J. Schoelkopf, *Phys. Rev. A* **76**, 042319 (2007).
- [28] T. Taneichi and T. Kobayashi, *J. Phys. Soc. Jpn.* **67**, 1594 (1998).
- [29] A. M. Fedotov, N. B. Narozhny, and Yu. E. Lozovik, *Phys. Lett. A* **274**, 213 (2000); N. B. Narozhny, A. M. Fedotov, and Yu. E. Lozovik, *Phys. Rev. A* **64**, 053807 (2001).
- [30] I. Carusotto, M. Antezza, F. Bariani, S. De Liberato, and C. Ciuti, *Phys. Rev. A* **77**, 063621 (2008).
- [31] M. Boissonneault, A. C. Doherty, F. R. Ong, P. Bertet, D. Vion, D. Esteve, and A. Blais, *Phys. Rev. A* **85**, 022305 (2012).
- [32] R. R. Puri, *Mathematical Methods of Quantum Optics* (Springer, Berlin, 2001).